Boundary-Layer Meteorol
https://doi.org/10.1007/s10546-018-0352-8

RESEARCH ARTICLE

Optimizing the Determination of Roughness Parameters for Model Urban Canopies

Pablo Huq[1] · **Auvi Rahman**[1]

Received: 10 February 2017 / Accepted: 3 April 2018

Abstract We present an objective optimization procedure to determine the roughness parameters for very rough boundary-layer flow over model urban canopies. For neutral stratification the mean velocity profile above a model urban canopy is described by the logarithmic law together with the set of roughness parameters of displacement height d, roughness length z_0, and friction velocity u_*. Traditionally, values of these roughness parameters are obtained by fitting the logarithmic law through (all) the data points comprising the velocity profile. The new procedure generates unique velocity profiles from subsets or combinations of the data points of the original velocity profile, after which all possible profiles are examined. Each of the generated profiles is fitted to the logarithmic law for a sequence of values of d, with the representative value of d obtained from the minima of the summed least-squares errors for all the generated profiles. The representative values of z_0 and u_* are identified by the peak in the bivariate histogram of z_0 and u_*. The methodology has been verified against laboratory datasets of flow above model urban canopies.

Keywords Displacement height · Friction velocity · Laboratory experiments · Rough boundary layer · Roughness length · Urban canopy flow

1 Introduction

The buildings and infrastructure of a city or urban area, together with features such as hills, lakes, parks and trees, form what is commonly termed the urban canopy (Oke 1987). Airflow through and above the urban canopy comprises a rough, turbulent boundary layer whose dynamics determines the turbulent transport of mass, momentum and scalars, such as heat,

✉ Auvi Rahman
auvi@udel.edu

Pablo Huq
huq@udel.edu

[1] College of Earth, Ocean, and Environment, University of Delaware, Newark, DE 19716, USA

Published online: 02 May 2018

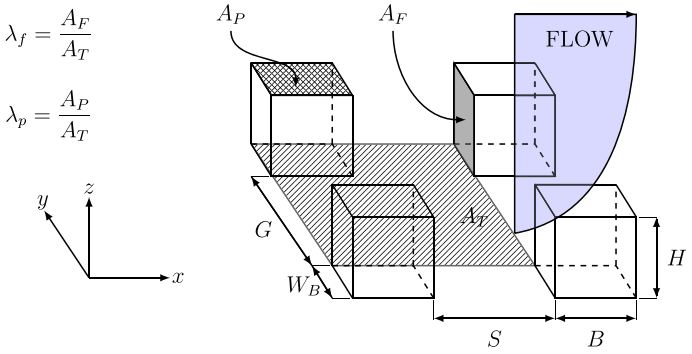

Fig. 1 Perspective view of a model urban canopy. Here, H, W_B and B are the height, width and depth of the building or roughness elements, S and G denote the longitudinal and lateral spacing between buildings, respectively, the shaded areas A_F, A_P are the frontal and plan areas of the buildings, respectively, and A_T is the total plan area of the buildings including the area between the buildings. The schematic portrays an aligned arrangement as opposed to a staggered model canopy where upstream and downstream buildings are offset laterally. Here, λ_p and λ_f are areal-density parameters. A typical boundary-layer velocity profile is depicted on the right-hand side

humidity and pollutants, which in turn affect the air quality and even the local weather in cities (Collier 2006). Reviews on boundary-layer flow above urban canopies are provided by Britter and Hanna (2003), Fernando (2010) and Barlow (2014). The prediction of the mean velocity profile, which is an essential step towards understanding urban canopy flow, is made difficult by the geometry and arrangement of buildings (i.e. the urban morphology) for which the results of laboratory experiments in wind and water tunnels (Yee et al. 2006), field studies (Roth 2000; Kent et al. 2017), and numerical modelling (Milliez and Carissimo 2007; Leonardi and Castro 2010) of flow in urban canopies provide a useful framework.

There has been an enormous effort to characterize the aerodynamic roughness of urban canopies, including the development of morphometric, anemometric and reference-based methods, with recent methods for determining urban-roughness parameters comprehensively reviewed by Kent et al. (2017). Macdonald et al. (1998) and Macdonald (2000) utilized morphometric approaches to delineate the characteristics of the profiles of mean velocity, and to develop models for the displacement height d and roughness length z_0 of model urban canopies by use of the fractional areal densities λ_p and λ_f, which are defined as the ratio of plan and frontal area to the total lot area, respectively (see Fig. 1). While areal densities have been used in describing the roughness characteristics of cities and urban areas (Grimmond and Oke 1999), they do not distinguish between aligned and staggered arrangements, nor do they address the impact of the variability of the building heights on the flow dynamics. Thus, the variance of height and other parameters, such as the aspect ratio H/W_B of building height H to building width W_B, are also found to be useful in the description of the urban environment (Shockling et al. 2006; Huq and Franzese 2013; Kanda et al. 2013). These numerous parameters reflect the complex ways that urban morphology influences the roughness, and the form of the mean velocity profile within and above urban canopies (Cheng and Castro 2002; Kastner-Klein and Rotach 2004).

The mean velocity profile within the canopy decays exponentially (Cionco 1965), whereas it is well described by the logarithmic velocity profile (Oke 1987)

$$U(z) = \frac{u_*}{\kappa} \ln\left(\frac{z-d}{z_0}\right), \tag{1}$$

above the canopy in neutral stratification. Here, z_0 is the aerodynamic roughness length, u_* is the friction velocity and κ is the von Kármán constant. As z_0 alone is often inadequate for accounting for the surface roughness of a tall canopy, a zero-plane displacement d (the displacement height hereafter) is introduced (Rossby and Montgomery 1935; Paeschke 1937; Raupach and Thom 1981; Stull 1988).

While there are similarities between the characteristics of boundary layers in urban canopies and rough walls or plates, there are also differences. The value of the ratio of the roughness-element scale z_0 to the depth δ of the rough-plate boundary layer is small ($z_0/\delta \ll 1$, see the reviews of Jimenez 2004; Flack et al. 2005). In contrast, the effects of buildings as roughness elements of the urban canopy are more pronounced, since the ratio H/δ of building height H to depth δ of atmospheric boundary layer can reach $\mathcal{O}(0.1)$ or more in winter months when the inversion level may descend below the rooftop level of tall buildings in cities. Therefore, the consequence of values of H/δ as large as $\mathcal{O}(0.1)$ on the scaling of rough boundary-layer flow requires further attention.

A salient feature of the urban canopy is its heterogeneity, which arises from buildings of different sizes and shapes and varying gaps between the buildings. While flow normal to buildings can result in zones of stagnation, long gaps between buildings in urban canopies form canyons where the flow is accelerated. Additionally, the sharp corners of buildings facilitate the generation of wakes. The presence of such dynamic flow features with different length and time scales complicates the estimation of roughness characteristics of urban canopies (Cheng and Castro 2002; Kastner-Klein and Rotach 2004; Castro et al. 2006). Turbulent exchange within the urban canopy and the flow above is also affected by the presence of the shear layer near the tops of buildings or roughness elements (Huq et al. 2007; Reynolds and Castro 2008).

An important step in the use of Eq. 1 is the determination of the displacement height d for which different methods have evolved (Mohammad et al. 2014), with the heterogeneous flow arising from wakes and canyons complicating the objective determination of the value of d. For boundary-layer flow above urban canopies, it is common to assume $d \approx H$, and typically taken as $d = 2H/3$ (Sogachev and Kelly 2016). We show that such a simple estimate of the displacement height yields poor results for urban canopy flows since d/H is not constant, but varies with the morphology of the canopy (Grimmond and Oke 1999), as discussed in Sect. 2.

There is agreement that the logarithmic law is useful for characterizing urban canopy flows (Amir and Castro 2011; Kent et al. 2017), but requires accurate estimates of the displacement height d, roughness length z_0, and friction velocity u_*. However, the lack of a consensus for the calculation of the displacement height is a problem. Therefore, we propose an objective optimization approach to determine the (roughness) parameters d, z_0 and u_* from the mean velocity profile.

2 Background

Knowledge of the flow over rough boundaries and plant canopies has been useful in the analysis of the urban boundary layer (Garratt 1994; Kaimal and Finnigan 1994). For example, the logarithmic velocity profile and the extinction relation described below, together with the effective characterization of roughness effects, provide tools with which to model the mean velocity profile above and within urban canopies. However, our understanding of flow over very rough surfaces is still incomplete (Sogachev and Kelly 2016), and the calculation

procedures for values of roughness parameters remain subjective. We review some pertinent background material of the urban boundary layer prior to introducing an objective approach for calculating the roughness parameters.

2.1 Vertical Structure of the Urban Boundary Layer

The division of the complex flow field into layers facilitates the analysis of urban boundary-layer flow. Closest to the ground is a roughness sublayer of depth of the order of the height H of the roughness elements (e.g. buildings). Customary practice is to sub-divide the roughness sublayer into two regions—the urban canopy layer comprising roughness elements, and the above-canopy roughness sublayer. The roughness sublayer is influenced by the dynamics of the flow over the roughness elements, and so the depth of each of its constituent layers is of the order of the height H of the roughness elements. A current focus of research is the examination of the spatial variability (i.e. inhomogeneity) of flow within the roughness sublayer. A complication arises for surface elements of height $H > \delta$ because of the suppression of the inertial sublayer, which is defined as the layer in which the flow has adjusted to the effects of the underlying roughness elements (Grimmond and Oke 2002; Britter and Hanna 2003). In this case, the roughness sublayer may dominate the dynamics of the coupling of the surface to the urban boundary layer aloft. Turbulence also influences transport in both roughness and inertial sublayers, for which observations show the turbulence to be inhomogeneous both vertically and horizontally in the former, and vertically homogeneous in the latter. These issues are discussed in detail by Barlow (2014).

2.2 Flow Within the Roughness Sublayer

The distribution of roughness elements comprising plant canopies is more homogeneous than the distribution of roughness elements in the urban canopy. Thus, it is surprising that the extinction profile defined below originally developed by Inoue (1963), Cionco (1965), Lettau (1969) and Thom (1971) to describe the decay of the spatially averaged mean velocity profile through a plant canopy, is also useful for characterizing the spatially-averaged mean velocity profile within the urban canopy layer (Macdonald 2000). The velocity profile within the canopy (i.e. $z \leq H$) is described by the exponential function (Cionco 1965)

$$U(z) = U(H) \exp\left[a\left(z/H - 1\right)\right], \tag{2}$$

where a is an attenuation coefficient. Equation 2 is referred to as the extinction profile.

2.2.1 Matching Velocity Profiles Above and Below the Urban Canopy

As the velocity profile in the urban boundary layer is continuous, it is necessary to match the velocity profiles below and above the urban canopy. The simplicity of the forms of the extinction relation and logarithmic law enables matching of the first derivatives of Eqs. 1 and 2 at the urban canopy height $z = H$ (Shinn 1971),

$$\frac{\mathrm{d}}{\mathrm{d}z}\left\{U_H \exp\left[-a\left(1 - \frac{z}{H}\right)\right]\right\}_{z=H} = \frac{\mathrm{d}}{\mathrm{d}z}\left[\frac{u_*}{\kappa}\ln\left(\frac{z-d}{z_0}\right)\right]_{z=H}, \tag{3}$$

where

$$a = \frac{u_*}{\kappa U_H\left(1 - d/H\right)}, \tag{4}$$

U_H is the mean velocity at $z = H$, and a is essentially the attenuation coefficient used in Cionco's relation for below-canopy flow (Eq. 2). In Eq. 4, when d/H is small, the value of a is small, resulting in reduced shear at the building height. Conversely, a larger value of d/H increases the value of a, giving higher levels of shear. Thus, the attenuation coefficient controls the form of the velocity profile, as can be seen more clearly by rewriting Eq. 4 as

$$d = H - \frac{u_* H}{a\kappa U_H}. \tag{5}$$

For present purposes, Eq. 5 shows that d varies with the flow parameters. Accurate values of d, z_0 and u_* are required for the prediction of the transport of momentum and scalars in urban canopies, and is made difficult by the essentially empirical and subjective procedure involved in evaluating d, z_0 and u_*. Thus, an objective algorithm to determine the functional dependence of the roughness parameters on the flow variables is introduced below.

2.3 Review of Methods to Determine the Roughness Parameters

Various methods exist with which to determine the roughness parameters (Mohammad et al. 2014) including morphometry, drag balance, and anemometry (turbulence measurements) methods.

2.3.1 Morphometric Methods

Estimation of the roughness parameters of the urban canopy is made difficult by the heterogeneous morphology. A pragmatic approach for determining the roughness parameters is through the use of areal packing densities λ_p and λ_f of the roughness elements (or buildings) comprising the urban canopy. Figure 1 illustrates the idea for a model urban canopy comprising buildings or roughness elements of uniform height in an aligned arrangement.

Macdonald et al. (1998) recognized the influence of the areal densities λ_p and λ_f in determining the roughness and drag of urban canopies. The plan-area packing density λ_p and frontal-area packing density λ_f are defined as $\lambda_p = A_P/A_T$ and $\lambda_f = A_F/A_T$, respectively. A sparse canopy has a small value of λ_p, whereas a large value reflects a dense canopy. Macdonald et al. (1998) delineated the role of areal densities λ_p and λ_f in determining the roughness from laboratory experiments on model urban canopies. The roughness length z_0 and displacement height d depend on the value of the areal density parameters, and also on the arrangement (e.g. aligned or staggered) of roughness elements and height variability. For uniform-height roughness elements, Macdonald et al. (1998) developed the expressions given below for the displacement height and roughness length by incorporating the obstacle drag into the analysis of Lettau (1969), who estimated $z_0/H = 0.5\lambda_f$,

$$\frac{d}{H} = 1 + A^{-\lambda_p}\left(\lambda_p - 1\right), \tag{6}$$

and

$$\frac{z_0}{H} = \left(1 - \frac{d}{H}\right)\exp\left\{-\left(0.5\frac{C_D}{\kappa^2}\left(1 - d/H\right)\lambda_f\right)^{-0.5}\right\}. \tag{7}$$

Here, C_D is a drag coefficient for which Macdonald et al. (1998) suggest a typical value of 1.2, with z_0 and d determined solely from geometric parameters. Such formulations are termed morphometric. The displacement height non-dimensionalized by the building height d/H increases monotonically with increasing plan density λ_p in approaching the building height

H. In contrast, the non-dimensional roughness length z_0/H evolves non-monotonically with frontal density λ_f. Drag and building wake losses cause the non-dimensional roughness length z_0/H to increase with frontal density λ_f for small λ_f. A very large canopy density λ_f causes the flow to skim over the canopy, which reduces the flow interaction with the buildings below (Oke 1987; Garratt 1994).

Such morphometric methods are clearly idealized approaches: for example, the scheme of Macdonald et al. (1998) does not include the possible role of λ_f in determining d. The simplicity of the scheme is attractive, and has yielded insights into the dynamics of flow in urban areas, as well as effective estimates of the roughness parameters in cities (Grimmond and Oke 1999).

Efforts have also been made to establish the impact of height variability on the roughness length z_0. Regressions relating the enhancement of the value of z_0 to the second moment of height variability (i.e. the root-mean-square height H') of topography have been developed by Shockling et al. (2006) and Kanda et al. (2013). Relations utilizing third-order moments (skewness) have been proposed by Flack and Schultz (2010) and Kawaguchi et al. (2011). A recent parametric study of the statistical moments of synthetic urban-like topography using large-eddy simulations (Zhu et al. 2017) confirms that both the second- and third-order moments of height variability are important in augmenting z_0, while fourth-order moments (kurtosis) are not. They also note that second-order moments of height variability influence the displacement height d. However, experiments need to be undertaken to corroborate these numerical results.

2.3.2 Drag Analysis

Roughness parameters can also be obtained from measurements of the drag force D of a model urban canopy with a drag balance in a wind tunnel. Data are presented as a non-dimensional drag coefficient C_D,

$$C_D = \frac{\tau}{0.5\rho U_H^2}, \tag{8}$$

where $\tau = D/A$, A is the roughness surface area, U_H is the reference velocity, and ρ is the density of air. The roughness length can be determined from the drag assuming the logarithmic velocity profile,

$$z_0 = (H - d)\exp\left[-\frac{\kappa}{\sqrt{0.5C_d}}\right]. \tag{9}$$

Hagishima et al. (2009) performed experiments with staggered and aligned canopy configurations in a wind tunnel using the drag-balance approach, as well as split-film anemometry to resolve the velocity profile. Values of C_D are similar (≈ 1.2) for aligned and staggered model canopies of uniform heights, with larger values found for canopies of non-uniform height, and also for flow directions 45° to the axis of the buildings and canyons.

2.3.3 Anemometric Methods

Approaches to determine the roughness parameters d, z_0 and u_* from velocity data belong to the class of anemometric methods for which best-fit graphical solution techniques are typically applied. Useful rules-of-thumb have evolved such as $d \approx 2H/3$ and $z_0 \approx H/10$ (e.g. Stull 1988; Garratt 1994; Foken 2008). A recent study for the companion problem of determining d and z_0 from single-level velocity data (as opposed to a velocity profile)

concludes that the comparison of results obtained from different methods can help yield more robust estimates (Graf et al. 2014). As the potential role of sparseness (or density) of roughness elements leads to uncertainties for both problems, the development of objective methodologies would be helpful.

3 Objective Methodology to Determine Roughness Parameters

For neutral stratification the procedure to calculate the roughness parameters requires measurements of the mean wind (flow) speed at different heights at a given site for calculating the logarithmic velocity profile according to Eq. 1, which in non-dimensional form is

$$\frac{U\,(z/H)}{U_H} = \frac{u_*/U_H}{\kappa} \ln\left(\frac{z/H - d/H}{z_0/H}\right). \tag{10}$$

While it is natural to use U_H as a scaling velocity, since it is an intrinsic scale of the flow field, the proposed optimization method is independent of the choice of the scaling (or reference) velocity. For example, another velocity scale could be the freestream velocity U_∞, but U_H is more attractive as it is more likely to be available, though the value of U_H will have some variability. With three unknowns (d, z_0, and u_*), estimates are usually obtained from a fitted velocity profile determined iteratively by trial and error, which is subjective, and so values obtained in practice vary (Grimmond and Oke 1999). An objective method enables comparisons of the roughness parameters obtained and available in the literature. We propose a new method to determine the roughness parameters for neutrally-stratified boundary-layer flow above an urban canopy using mean velocity data assuming an incompressible fluid, the validity of the logarithmic law above the canopy, and the constraint of the displacement height d between zero and H.

Our rationale for these assumptions is primarily convenience, as we seek to examine the utility of the proposed methodology for the simple case of a horizontally-homogeneous boundary-layer flow. The domain of the constraint can be extended to $d/H > 1$ for heterogeneous canopies. Since the results of Hagishima et al. (2009) and Zaki et al. (2011) show that the displacement height d can exceed the average building height $\overline{H}$ in heterogeneous urban areas, the constraint of $0 \leq d \leq H$ may need to be relaxed to account for, e.g., the tallest building in the region.

The value of the von Kármán constant κ needs discussion. Recent surveys of measurements give values in the range $0.37 - 0.43$, suggesting a dependence on the type of flow (Smits et al. 2011). For example, $\kappa = 0.421$ for high Reynolds number pipe flow (McKeon et al. 2004), but $\kappa = 0.387$ for atmospheric surface-layer flow in polar regions (Andreas et al. 2006). We use a value of $\kappa = 0.4$ for calculations here. A different value of κ only changes the value of the friction velocity u_* without affecting the value of the displacement height d or roughness length z_0.

We introduce a framework to calculate values of the roughness parameters by constructing an ensemble of parameter values determined from a single mean velocity profile. The method provides a distribution of estimates rather than just a single value.

3.1 Obtaining Multiple Velocity Profiles from a Single Velocity Profile

A schematic of the procedure for generating multiple profiles by selecting subsets of data points from the original profile of velocity data points is shown in Fig. 2. For the data above the canopy, we consider any combination of the data points to be a unique mean velocity

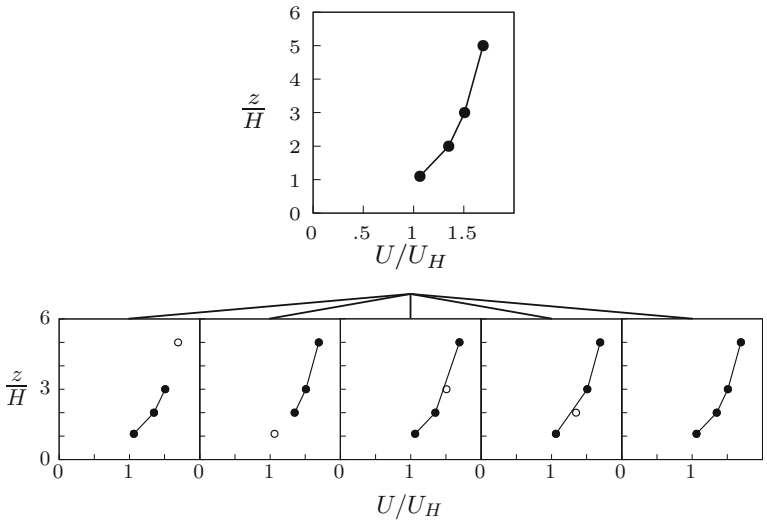

Fig. 2 Schematic of the generation of subsets of profiles from the original profile. The top panel shows the original velocity profile comprising four data points. The lower panels show multiple velocity profiles derived from the original profile by selecting subsets from the original profile

profile. For our purposes, the lowermost data point is thus selected to be the closest one above the roughness-element height. For the analysis described in Sect. 4, the location of the lowest point is $1.09H$ and $1.01H$ for the datasets of Macdonald et al. (2000) and Castro et al. (2006), respectively. The optimization methodology utilizes all data above the roughness-element height H, with data below H discarded. In our method, we consider all profile combinations with a minimum of three measurement heights. Thus, for a total number n of available data points, we choose all the k different data points, where $k \geq 3$, and obtain an ensemble of mean velocity profiles. The total number of possible profiles N_G can be computed as a summation of the different number of combinations with at least three data points,

$$N_G = \sum_{k=3}^{n} \binom{n}{k}, \tag{11}$$

where $\binom{n}{k} = \frac{n!}{k!(n-k)!}$. The number of combinations and, hence, the number of generated profiles, increases rapidly with the number of measurement heights. Even few data points generate many profiles; for example, 10 data points yield 968 profiles. Each generated profile is analyzed to evaluate the values of its roughness parameters by utilizing a least-squares procedure described in detail below. As application of the optimization methodology for profiles with a large number of points becomes computationally onerous, approaches that expedite the computation become necessary, such as increasing the minimum number of points for a generated profile to be >3.

3.2 Least-Squares Procedure to Determine Roughness Parameters from a Single Profile

The proposed optimization approach yields the set of roughness parameters d, z_0 and u_* related through the logarithmic law (Eq. 1). Such non-linear equations can be solved itera-

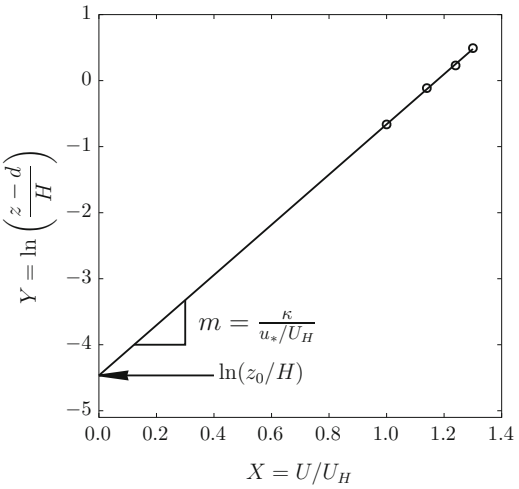

Fig. 3 Schematic of the fitting procedure of a profile with four data points for a given value of the displacement height. The minimum error occurs when the fit is a straight line. The value of the friction velocity is obtained from the slope of this straight line, and the roughness length is obtained from the intercept of the straight line with the ordinate

tively using standard statistical packages. However, this requires the added burden of initial values that have to be guessed. Iterative optimization methods can be avoided by transforming the non-linear equation into a linear form to simplify the optimization procedure as shown below.

The experimental data have to be fitted to the non-dimensional logarithmic law to obtain the roughness parameters, which involves the minimization of errors utilizing the least-squares procedure. While non-dimensionalization is not necessary, it has the advantage of simplifying the assessment of the relative magnitudes of roughness parameters to the canopy scales (e.g. z_0/H, u_*/U_H, etc.). First, we derive an equation of the linear form $Y = mX + C$ by rearranging Eq. 10 to

$$\underbrace{\ln\left(\frac{z-d}{H}\right)}_{Y} = \underbrace{\frac{\kappa}{u_*/U_H}}_{m}\ \underbrace{\frac{U\,(z/H)}{U_H}}_{X} + \underbrace{\ln\left(\frac{z_0}{H}\right)}_{C}, \tag{12}$$

where $Y = \ln\left(\frac{z-d}{H}\right)$ is the ordinate, $m = \frac{\kappa}{u_*/U_H}$ is the slope, $X = \frac{U(z/H)}{U_H}$ is the abscissa and $C = \ln\left(\frac{z_0}{H}\right)$ is the intercept on the ordinate. The least-squares procedure is performed on a plot such as that displayed in Fig. 3, with $\ln\left(\frac{z-d}{H}\right)$ as the ordinate and $\frac{U(z/H)}{U_H}$ as the abscissa. The non-dimensional friction velocity u_*/U_H is obtained from the slope m of the line of best fit, and the non-dimensional roughness length z_0/H is obtained from the exponent of the intercept C. The equations for the least-squares procedure are provided in the Appendix.

The least-squares procedure involves minimizing the error between the measured Y_{meas} and estimated Y_{est} values of the ordinate $\ln\left(\frac{z-d}{H}\right)$, where E is the minimized error from the least-squares procedure to obtain the best-fit line for a generated profile corresponding to $Y = mX + C$,

$$\begin{aligned} E &= \sum (Y_{meas} - Y_{est})^2 \\ &= \sum (Y_{meas} - m_{est} X_{meas} - C_{est})^2 \\ &= \sum_{i=1}^{k} \left[\ln\left(\frac{z_{i,\text{meas}} - d}{H}\right) - \frac{\kappa}{u_{*,\text{est}}/U_H} \frac{U_{i,\text{meas}}}{U_H} - \ln\left(\frac{z_{0,\text{est}}}{H}\right) \right]^2 . \end{aligned} \tag{13}$$

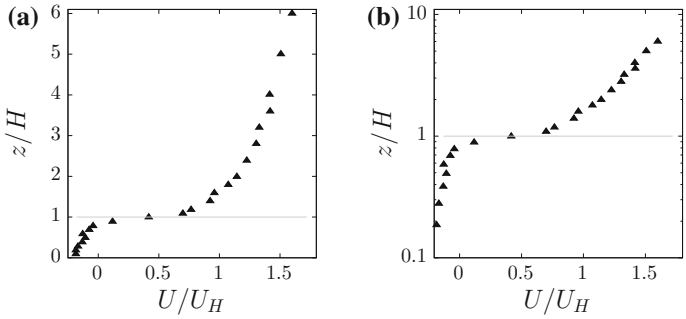

Fig. 4 Mean-velocity-profile data from Macdonald et al. (2000) in linear (panel **a**) and logarithmic–linear (panel **b**) coordinates. The thin grey horizontal line in both panels marks the top of the roughness element at $z = H$, there are 13 data points above the roughness elements, and U_H is a reference velocity upstream of the model canopy at $z = H$

The above approach has evolved from the standard representation of velocity-profile data with height on the ordinate and velocity on the abscissa (e.g. Stull 1988).

3.3 Determination of the Optimal Value of the Displacement Height

A single value of d/H produces least-squares errors (E) for each of the generated profiles with the sum of these errors then determined for all the profiles. This is repeated for a sequence of values of d/H from the ground to the top of the canopy, with the representative value of d/H associated with the minimum sum. The steps of the methodology are demonstrated by analyzing the mean-velocity-profile data from Macdonald et al. (2000) as shown in Fig. 4, where there are 13 data points above the canopy. The details of the experiment, as well as a further discussion of Fig. 4, are given in Sect. 4. The 13 data points generate 8,100 profiles, and the least-squares procedure for each of the 8,100 generated profiles is performed for a specific value of d/H, with 8,100 sets of $\{z_0/H, u_*/U_H, E\}$ obtained. The summed error S is obtained by adding all 8,100 values of E,

$$S(d/H) = \sum_{i=1}^{N_G} E_i, \tag{14}$$

where N_G is the total number of generated profiles (i.e. $N_G = 8100$ for the example case). Values of S are obtained by repeating this procedure for a sequence of values of d/H by varying d/H from zero to one in incremental steps of $\Delta d/H$, with the exact value depending on the resolution requirements. We use a $\Delta d/H$ value of 0.01, which divides H into 100 steps with 101 values of d/H; 100 steps is also practical in terms of computational resources. Figure 5 shows the S versus d/H curve plotted using these 101 sets of values of (d/H, S). The d/H value associated with the minima of the S versus d/H curve is defined as the representative value of the displacement height of the measured profile. Thus, Eq. 14 is the objective function of the optimization methodology. The representative value of the displacement height for the Macdonald et al. (2000) dataset occurs at the minimum $d/H = 0.75$ in the example of Fig. 5.

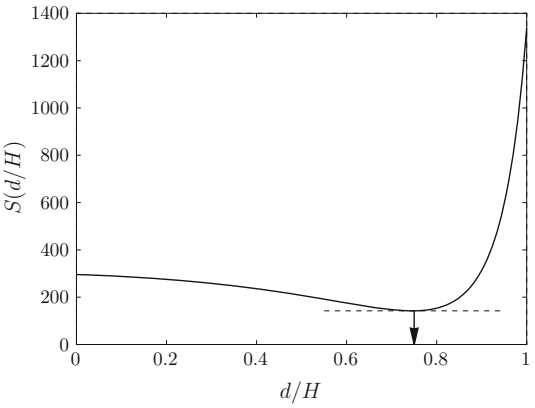

Fig. 5 The variation of S for different values of d/H. The vertical and horizontal axes correspond to the summed error S and the sequence of values of d/H from zero to one. The curve is generated by processing the data described in Macdonald et al. (2000). The minimum of the curve is marked by the horizontal tangent. The optimal d/H value is marked by the downwards pointing arrow

3.4 Determination of the Optimal Value of the Roughness Length and Friction Velocity

There are 8,100 sets of values of roughness length z_0/H and friction velocity u_*/U_H associated with the representative value of d/H used in the histograms and bivariate histogram of z_0/H and u_*/U_H in Fig. 6, with the ordinate representing the frequency of occurrence. The representative values ($z_0/H = 0.041$ and $u_*/U_H = 0.132$) of the roughness length z_0/H and friction velocity u_*/U_H are associated with the tallest bin (i.e. the most frequent) in the bivariate histogram. The set $(d/H, z_0/H, u_*/U_H)$ of representative values of the roughness parameters of the Macdonald et al. (2000) dataset is used for the analysis in Sect. 4.

4 Testing of Optimization Methodology Against Laboratory Datasets

We analyze data of mean velocity profiles of neutrally-stratified flow over model urban canopies measured in laboratory experiments to evaluate the optimization methodology. The evaluation of published datasets with sufficient measurements of individual velocity profiles, both above and within the canopy, include those of Macdonald et al. (2000) (also reported by Hanna et al. 2002) and Castro et al. (2006), which were obtained from experiments in water and wind tunnels, respectively. Experiments were undertaken using model urban canopies with both aligned and staggered arrangements of roughness elements by Macdonald et al. (2000) and Castro et al. (2006). We analyze velocity profiles taken in the middle of the wake region behind a roughness element in the aligned canopy configuration of Macdonald et al. (2000) and the staggered configuration of Castro et al. (2006). The flow in both water- and wind-tunnel experiments described above is fully adjusted or evolving very slowly as the fetch or location of the profile is greater than the minimum fetch recommended by Wieringa (1993). For both sets of experiments, the value of H/δ (roughness height H and depth δ of the boundary layer) is 0.13. The flow fields above such model urban canopies represent very rough boundary layers.

Macdonald et al. (2000) conducted experiments at the University of Waterloo in a water tunnel 1.2 m high, 1.2 m wide, and 12.8 m long, with a test section 2.4 m long, and a flow depth of 800 mm. Velocity measurements were obtained using a micro-acoustic Doppler velocimeter, with boundary-layer development promoted by a Counihan vortex generator (Counihan 1969). The model canopy comprised 50 mm ($= H$) cubic roughness elements

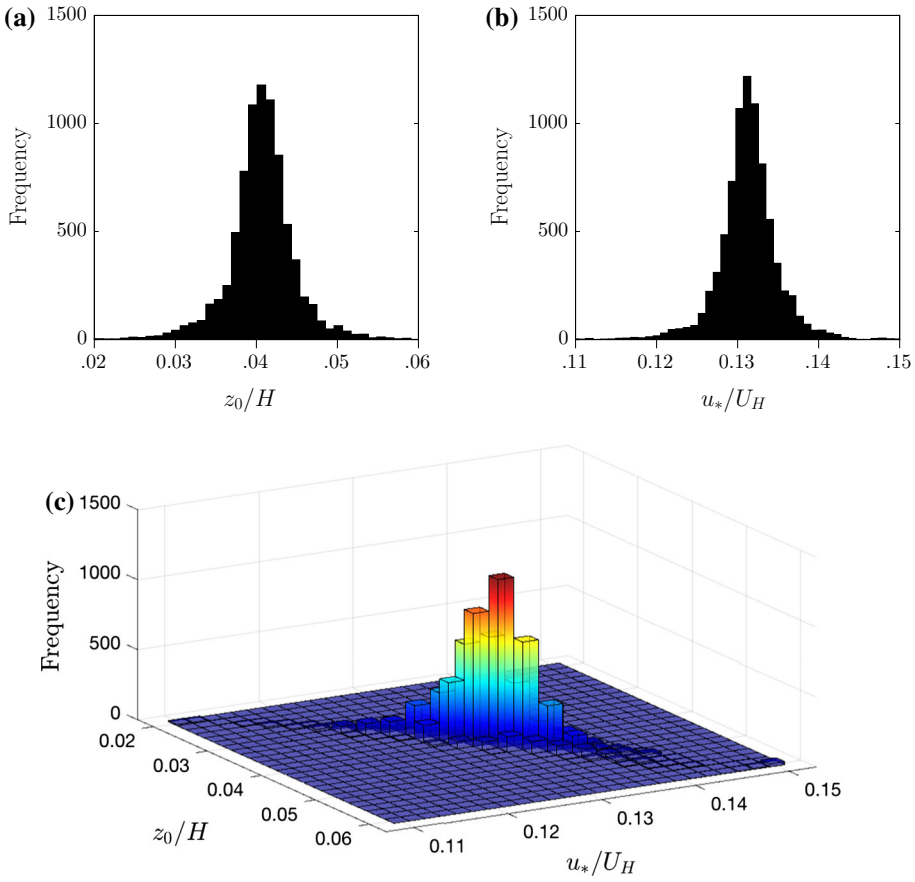

Fig. 6 Individual and bivariate histograms of the roughness length z_0/H and friction velocity u_*/U_H. Panel **a** shows the histogram of z_0/H, and panel **b** shows the histogram of u_*/U_H. Panel **c** shows the bivariate histogram of z_0/H and u_*/U_H. The representative values of z_0/H and u_*/U_H are given by the peak of the bivariate histogram

arranged in a square (i.e. aligned) configuration, and the gap between roughness elements was $1.5H$ ($= 75$ mm) in both the direction of (S) and transverse (G) to the flow (see Fig. 1). Velocity-profile data were obtained > 1 m from the start of the canopy at half a cube scale behind the back face of row nine of the model urban canopy. Values of the areal parameters are 0.16 for both λ_p and λ_f, and an aspect ratio $H/W_B = 1$. We utilize the reported data up to $z/H = 6$, with the depth δ of the boundary layer reported to be 0.4 m. The reference velocity U_H defined as the mean velocity upstream of the model urban canopy at height H is 50.5 mm s^{-1}, giving a Reynolds number $U_H H/\nu$ of about 2500. Other Reynolds numbers given by Macdonald et al. (2000) based on values of the roughness length z_0, friction velocity u_* and half width $W/2$ of the tunnel are $Re_* = u_* z_0/\nu \approx 10$ and $Re_\tau = W u_*/(2\nu) \approx 4000$; Macdonald et al. (2000) also reported values of $d/H = 0.33$, $z_0/H = 0.1$ and $u_*/U_H = 0.162$.

The experiments of Castro et al. (2006) were conducted at the University of Southampton in a low-speed wind tunnel with a test section 600 mm high, 900 mm wide and 4.5 m

long. Most of the velocity measurements were obtained using hot-wire anemometry, with the friction velocity u_* determined from pressure tappings. Cubes of 20 mm ($= H$) were arranged in a staggered configuration to form the model urban canopy. Castro et al. (2006) reported details of individual velocity profiles at four different locations within the canopy, as well as an averaged mean velocity profile for a model urban canopy comprising the cubes. We analyze their P_1 profile, which is located in the wake region about half a cube scale from the back face of the cube positioned 3 m downstream from the start of the model urban canopy. Values of the areal parameters are 0.25 for both λ_p and λ_f, the aspect ratio of height to width H/W_B is 1, and the gap between the roughness elements is 20 mm (i.e. $S = G = H$). Data were recorded up to $z/H \approx 2.2$, while the depth δ of the boundary layer is 0.148 m. The freestream velocity is 10 m s^{-1}, and the velocity U_H at the top of the model urban canopy is 1.58 m s^{-1}, yielding Reynolds numbers of $Re_H = U_H H/\nu = 2100$, $Re_* = u_* z_0/\nu = 5.1$ and $Re_\tau = W u_*/(2\nu) \approx 20000$. The reported non-dimensional displacement heights are $d/H = 0.85$, $z_0/H = 0.055$ and $u_*/U_H = 0.44$. Both Macdonald et al. (2000) and Castro et al. (2006) report mean flow speeds accurate to within 1% of the true value.

We now analyze two velocity profiles from the experiments described above to test the optimization methodology. The first step is to determine the average height of the model canopy and the mean velocity U_H at the average canopy height, which is straightforward for these model canopies comprising uniform-height cubic roughness elements. Subsequently, we utilize the velocity-profile data to determine optimized values of non-dimensional roughness parameters (d/H, z_0/H, u_*/U_H) by following the procedures described in Sect. 3. We then plot the profile using the optimized values and compare with the reported velocity profile.

Figure 4 shows the data of Macdonald et al. (2000) in non-dimensional form in linear and semi-logarithmic coordinates, with the ordinate and abscissa non-dimensionalized by the building height and the velocity at the building height, respectively. The top of the canopy is $z/H = 1$, which is delineated by the thin grey line. The data points above the canopy show that the magnitudes of the velocity profile increase in a manner consistent with a boundary layer extending to $z/H = 6$. Within the canopy (i.e. $z/H < 1$), the magnitudes of the velocity decrease. Negative values of the mean velocity occur for $z/H < 0.8$, which is consistent with the presence of recirculation in the wake region behind the roughness element.

For the Macdonald et al. (2000) dataset, the optimization methodology yields the set of roughness values $d/H = 0.75$, $z_0/H = 0.041$ and $u_*/U_H = 0.132$, which are 2.3, 0.4 and 0.8 times the values reported by Macdonald et al. (2000), respectively. The histograms for the data of Castro et al. (2006), which were similarly developed but are not shown here for brevity, yield values of $d/H = 0.96$, $z_0/H = 0.011$, $u_*/U_H = 0.306$, corresponding to 1.1, 0.2, and 0.7 times their respective reported values. Below, we show that the values of the set of roughness parameters determined from the optimization methodology result in improved fits to the reported velocity profiles of both sets of experiments. Note also that the values of d/H for both datasets differ from the common estimate $d/H \approx 2/3$.

The velocity profiles generated using optimized values of roughness parameters are compared with the reported velocity profiles as shown in Fig. 7. Note that while the scaling or reference velocity for these datasets is U_H, there are different definitions of U_H. For Macdonald et al. (2000), U_H is defined as the flow speed upstream of the canopy where the flow is unobstructed at height H. As Castro et al. (2006) did not report an upstream value of U_H, we determined a value of U_H at the top the roughness element within their canopy as the scaling parameter, with the consequence that, in Fig. 7, the value of U/U_H at $z/H = 1$ differs for the two datasets: $U/U_H < 1$ for the dataset of Macdonald et al. (2000) and $U/U_H = 1$ for the dataset of Castro et al. (2006). It is evident that the profile using optimized values (solid

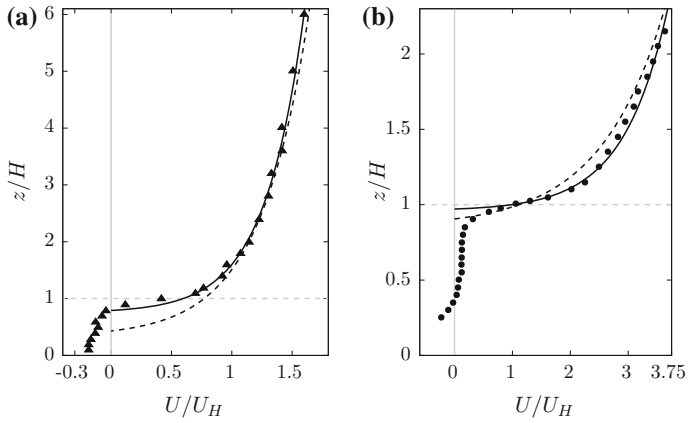

Fig. 7 Comparison of velocity profiles fitted with optimized and reported values of roughness parameters to measured experimental data. The solid curves are velocity profiles using optimized roughness parameters, and dashed curves are fits using the reported values of the roughness parameters. The horizontal dashed line at $z/H = 1$ shows the top of the roughness elements. Panel **a** shows data and velocity profiles for the experiments of Macdonald et al. (2000), and panel **b** shows data and velocity profiles for experiments reported by Castro et al. (2006). Here, U_H is a reference velocity at a height H upstream of the model urban canopy for Macdonald et al. (2000), but the velocity at height H within the model canopy for Castro et al. (2006)

line) is a better fit than the reported profiles shown by the dashed lines. The forms of the profiles within the canopy (i.e. $z/H < 1$) differ since negative values of U/U_H occur below $z/H = 0.8$ for the data of Macdonald et al. (2000), and only below $z/H = 0.3$ for Castro et al. (2006). Differences in the locations of negative values of U/U_H suggest the presence of different recirculation patterns behind the roughness elements within the canopy for aligned and staggered arrangements of roughness elements.

Another representation of the above-canopy mean velocity data is a semi-logarithmic plot with non-dimensional velocity $U^+ = U/u_*$ as the ordinate, and the distance from the wall expressed in wall units $y^+ = (z-d)u_*/\nu$ as the abscissa. On such a plot, the laminar sublayer occurs for small values $y^+ \approx 10$, with the logarithmic scaling region extending from near the top of the roughness elements to $y^+ \approx 1000$. A longstanding issue is the origin of coherent motions and structures in boundary-layer flows, as these control the transport towards and away from the boundary. A consensus is that the principal contribution to the production occurs close to the boundary at low Reynolds numbers, but within the logarithmic region at larger Reynolds numbers (Smits et al. 2011). Thus, there is interest in both the onset and extent of the logarithmic law, which can also be determined from Fig. 8. As the logarithmic law is valid above the model urban canopy height H, only data above the urban canopy are shown. Logarithmic-law fits are drawn through both datasets using optimized (solid circles and triangles) and reported (open circles and triangles) values of roughness parameters. Arrowheads on the abscissa with solid and dashed lines mark the top of the roughness elements at $y^+ = 25.8$ and $y^+ = 83$ for the optimized, and $y^+ = 140$ and $y^+ = 274$ for the reported values.

The range or extent of the logarithmic-law fit to the data with the optimized roughness parameters is almost twice that reported by Macdonald et al. (2000) and Castro et al. (2006), which, concomitant to the improved fits to the profiles of Fig. 7, illustrates the extended range of the logarithmic law, with the onset occurring from near the top of the roughness elements.

Also of interest is the fraction of the boundary-layer depth δ occupied by the logarithmic region for these very rough boundary-layer flows, which is determined from the largest value of y^+ in Fig. 8. We find that for the data of Macdonald et al. (2000), the logarithmic region

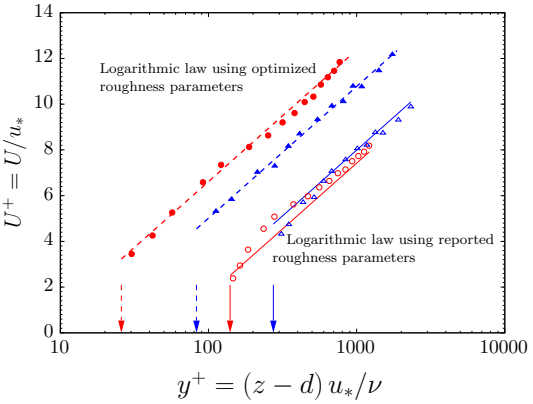

Fig. 8 Semi-logarithmic plot of U^+ against y^+. Red circles (both solid and open) and blue triangles (both solid and open) denote measurements reported by Castro et al. (2006) and Macdonald et al. (2000), respectively. The dashed lines depict the logarithmic law using optimized values of roughness parameters (d, z_0, u_*); the solid lines depict the logarithmic law using reported values of roughness parameters. The dashed vertical arrows mark the top of the roughness elements of the model urban canopies using optimized roughness parameters; the solid vertical arrows mark the top of the roughness elements using reported roughness parameters

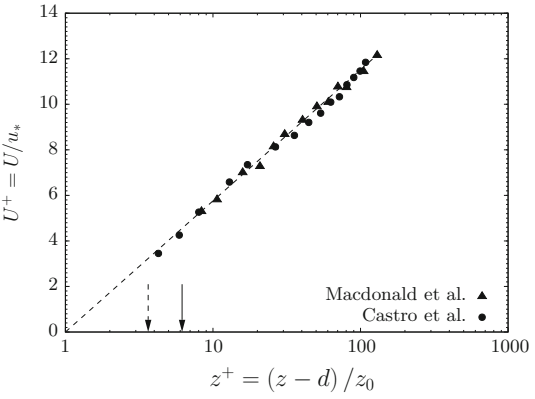

Fig. 9 Semi-logarithmic plot of U^+ against z^+. Scaling by z^+ collapses the experimental data. The dashed and solid vertical arrows mark the top of the roughness elements of the model urban canopies of Castro et al. (2006) and Macdonald et al. (2000), respectively

occupies more than 50% of the depth δ of the boundary layer, and that the fraction is smaller ($\approx 20\%$) for the data of Castro et al. (2006). We attribute the difference to the limited vertical extent of the traverse in that experiment. A large fraction of approximately 25% was also found by Cheng et al. (2007) for their very rough boundary-layer experiments. An emerging characteristic of very rough boundary-layer flows with $H/\delta = \mathcal{O}(0.1)$ is that the logarithmic region can occupy a substantial fraction of the boundary layer.

Note that the abscissa of Fig. 8 is the distance $(z-d)$ non-dimensionalized by the viscous scale ν/u_*. For very rough wall boundary-layer flows, Townsend (1980) suggests that the dimensionless distance from the boundary based on the roughness scale z_0 as $z^+ = (z-d)/z_0$ is likely to be useful for large z and u_*z/ν. Amir and Castro (2011) examined z_0 scaling, and found this collapses mean velocity data of U/u_* up to $z^+ \approx 60$ for flows over different kinds of surface roughness, including urban canopies comprising cubic roughness elements. A semi-logarithmic plot of U/u_* in terms of z_0 scaling is shown in Fig. 9, where we use

values of d, z_0 and u_* determined from the optimization methodology. The effectiveness of the z_0 scaling is evident as data collapse well over the range from $z^+ \approx 6$ for the experiment of Macdonald et al. (2000), and $z^+ \approx 4$ for the experiment of Castro et al. (2006) up to $z^+ \approx 150$. The range of the collapse of the logarithmic law is greater with the use of optimized surface-roughness parameters similar to Fig. 8.

5 Conclusion

The presented optimization methodology constitutes an objective procedure for determining the set of roughness parameters (d, z_0, and u_*) from samples of a mean velocity profile for boundary-layer flow over model urban canopies. Rather than finding a value arising from fitting the logarithmic law to the profile, the method provides distributions of roughness parameters generated by constructing velocity profiles from subsets of the total number of data points of the original profile. These profiles are systematically analyzed by incrementally varying the value of the displacement height from the ground to the top of the canopy. The roughness length and friction velocity are obtained by a least-squares fitting procedure for all the profiles. The representative value of the displacement height d is associated with the minima of the summed least-squares errors for all the profiles, with representative values of the roughness length z_0 and friction velocity u_* obtained from the bivariate histogram of z_0 and u_*. The methodology is effective as few data points are required to generate a sufficient number of subsets and profiles.

The procedure has been tested with data collected from water and wind tunnels with model urban canopies. The values of the areal parameters of these model urban canopies are $\lambda_\mathrm{p} = \lambda_\mathrm{f} = 0.15$ and 0.25 for the water- and wind-tunnel experiments, respectively. The ratio H/δ of both canopies is 0.13. The optimization methodology yields values of roughness parameters giving improved fits to the measured velocity data of both experiments. For these very rough boundary-layer flows, the methodology identifies the onset of the logarithmic law to be close to the top of the model urban canopy, and extending one and a half decades corresponding to values $y^+ = \mathcal{O}(10^3)$. Hence, the logarithmic law occupies a substantial fraction ($> 50\%$) of the depth of the boundary layer. We also find the relevant length scale for collapsing the experimental data to be the roughness length z_0, rather than the viscous scale ν/u_*.

The optimization methodology enables the accurate and robust determination of the roughness parameters (d, z_0, u_*) for complex three-dimensional flow of model urban canopies. A useful next step would be to test the methodology against field data of urban canopies over cities and urban areas.

Appendix

The equations involved in the least-squares procedure for determining the friction velocity and roughness length are presented here. The friction velocity u_*/U_H is obtained from the slope

$$m = \left[\frac{\sum \left(\left(\ln \left(\frac{z-d}{H} \right) \right) \left(\frac{U(z/H)}{U_H} \right) \right) - \frac{\left(\sum \ln \left(\frac{z-d}{H} \right) \right) \left(\sum \frac{U(z/H)}{U_H} \right)}{k}}{\sum \left(\frac{U(z/H)}{U_H} \right)^2 - \frac{\left(\sum \frac{U(z/H)}{U_H} \right)^2}{k}} \right], \tag{15}$$

and the non-dimensional friction velocity $u_*/U_H = \kappa/m$, thus

$$\frac{u_*}{U_H} = \kappa \left[\frac{\sum \left(\left(\ln \left(\frac{z-d}{H} \right) \right) \left(\frac{U(z/H)}{U_H} \right) \right) - \frac{\left(\sum \ln \left(\frac{z-d}{H} \right) \right) \left(\sum \frac{U(z/H)}{U_H} \right)}{k}}{\sum \left(\frac{U(z/H)}{U_H} \right)^2 - \frac{\left(\sum \frac{U(z/H)}{U_H} \right)^2}{k}} \right]^{-1}, \tag{16}$$

and the roughness length z_0/H is obtained from the intercept

$$C = \left[\frac{\sum \ln \left(\frac{z-d}{H} \right)}{k} - \frac{\kappa}{u_*/U_H} \frac{\sum \frac{U(z/H)}{U_H}}{k} \right], \tag{17}$$

and the non-dimensional roughness length $z_0/H = \exp(C)$, thus

$$\frac{z_0}{H} = \exp \left[\frac{\sum \ln \left(\frac{z-d}{H} \right)}{k} - \frac{\kappa}{u_*/U_H} \frac{\sum \frac{U(z/H)}{U_H}}{k} \right], \tag{18}$$

where Σ represents a summation, and k is the number of data points for a profile.

References

Amir M, Castro IP (2011) Turbulence in rough-wall boundary layers: universality issues. Exp Fluids 51(2):313–326

Andreas EL, Claffey KJ, Jordan RE, Fairall CW, Guest PS (2006) Evaluations of the von Kármán constant in the atmospheric surface layer. J Fluid Mech 559:117–149

Barlow JF (2014) Progress in observing and modelling the urban boundary layer. Urban Clim 10:216–240

Britter R, Hanna S (2003) Flow and dispersion in urban areas. Annu Rev Fluid Mech 35(1):469–496

Castro IP, Cheng H, Reynolds R (2006) Turbulence over urban-type roughness: deductions from wind-tunnel measurements. Boundary-Layer Meteorol 118(1):109–131

Cheng H, Castro IP (2002) Near wall flow over urban-like roughness. Boundary-Layer Meteorol 104(2):229–259

Cheng H, Hayden P, Robins AG, Castro IP (2007) Flow over cube arrays of different packing densities. J Wind Eng Ind Aerodyn 95(8):715–740

Cionco RM (1965) A mathematical model for air flow in a vegetative canopy. J Appl Meteorol 4(4):517–522

Collier CG (2006) The impact of urban areas on weather. Q J R Meteorol Soc 132(614):1–25

Counihan J (1969) An improved method of simulating an atmospheric boundary layer in a wind tunnel. Atmos Environ 3(2):197–200

Fernando H (2010) Fluid dynamics of urban atmospheres in complex terrain. Annu Rev Fluid Mech 42:365–389

Flack K, Schultz M (2010) Review of hydraulic roughness scales in the fully rough regime. J Fluids Eng 132(4):041203

Flack KA, Schultz MP, Shapiro TA (2005) Experimental support for Townsend's Reynolds number similarity hypothesis on rough walls. Phys Fluids 17(3):035102

Foken T (2008) Micrometeorology. Springer, Berlin

Garratt JR (1994) The atmospheric boundary layer. Cambridge University Press, Cambridge, UK

Graf A, Boer A, Moene A, Vereecken H (2014) Intercomparison of methods for the simultaneous estimation of zero-plane displacement and aerodynamic roughness length from single-level eddy-covariance data. Boundary-Layer Meteorol 151(2):373–387

Grimmond CSB, Oke TR (1999) Aerodynamic properties of urban areas derived from analysis of surface form. J Appl Meteorol 38(9):1262–1292

Grimmond CSB, Oke TR (2002) Turbulent heat fluxes in urban areas: observations and a local-scale urban meteorological parameterization scheme (LUMPS). J Appl Meteorol 41(7):792–810

Hagishima A, Tanimoto J, Nagayama K, Meno S (2009) Aerodynamic parameters of regular arrays of rectangular blocks with various geometries. Boundary-Layer Meteorol 132(2):315–337

Hanna SR, Tehranian S, Carissimo B, Macdonald RW, Lohner R (2002) Comparisons of model simulations with observations of mean flow and turbulence within simple obstacle arrays. Atmos Environ 36:5067–5079

Huq P, Franzese P (2013) Measurements of turbulence and dispersion in three idealized urban canopies with different aspect ratios and comparisons with a Gaussian plume model. Boundary-Layer Meteorol 147:103–121

Huq P, Carrillo A, White LA, Redondo J, Dharmavaram S, Hanna SR (2007) The shear layer above and in urban canopies. J Appl Meteorol Clim 46:368–376

Inoue E (1963) On the turbulent structure of airflow within crop canopies. J Meteorol Soc Jpn Ser II 41(6):317–326

Jimenez J (2004) Turbulent flow over rough walls. Annu Rev Fluid Mech 36:173–196

Kaimal JC, Finnigan JJ (1994) Atmospheric boundary layer flows: their structure and measurement. Oxford University Press, New York, p 289

Kanda M, Inagaki A, Miyamoto T, Gryschka M, Raasch S (2013) A new aerodynamic parametrization for real urban surfaces. Boundary-Layer Meteorol 148(2):357–377

Kastner-Klein P, Rotach MW (2004) Mean flow and turbulence characteristics in an urban roughness sublayer. Boundary-Layer Meteorol 111(1):55–84

Kawaguchi Y, Senda T, Ando H, Kawashima H, Iwamoto K, Motozawa M, Ito T, Matsumoto A, Ito T (2011) Experimental investigation on effects of surface roughness geometry affecting to flow resistance. In: ASME-JSME-KSME 2011 joint fluids engineering conference. ASME, New York, pp 3945–3954

Kent CW, Grimmond S, Barlow J, Gatey D, Kotthaus S, Lindberg F, Halios CH (2017) Evaluation of urban local-scale aerodynamic parameters: implications for the vertical profile of wind speed and for source areas. Boundary-Layer Meteorol 164(2):183–213

Leonardi S, Castro IP (2010) Channel flow over large cube roughness: a direct numerical study. J Fluid Mech 651:519–539

Lettau H (1969) Note on aerodynamic roughness-parameter estimation on the basis of roughness-element description. J Appl Meteorol 8(5):828–832

Macdonald RW (2000) Modelling the mean velocity profile in the urban canopy layer. Boundary-Layer Meteorol 97(1):25–45

Macdonald RW, Griffiths RF, Hall DJ (1998) An improved method for the estimation of surface roughness of obstacle arrays. Atmos Environ 32(11):1857–1864

Macdonald RW, Carter S, Slawson PR (2000) Measurements of mean velocity and turbulence statistics in simple obstacle arrays at 1:200 scale. Thermal Fluids Report 2000-1, Department of Mechanical Engineering, University of Waterloo

McKeon BJ, Li J, Jiang W, Morrison JF, Smits AJ (2004) Further observations on the mean velocity distribution in fully developed pipe flow. J Fluid Mech 501:135–147

Milliez M, Carissimo B (2007) Numerical simulations of pollutant dispersion in an idealized urban area, for different meteorological conditions. Boundary-Layer Meteorol 122(2):321–342

Mohammad A, Zaki S, Hagishima A, Ali M (2014) Determination of aerodynamic parameters of urban surfaces: methods and results revisited. Theor Appl Climatol 122(3–4):635–649

Oke TR (1987) Boundary layer climates, 2nd edn. Routledge, London

Paeschke W (1937) Experimentelle untersuchungen zum rauhigkeits und stabilitaets-problem in der freien atmosphere. Beitr Phys Atmos 24:163–189

Raupach M, Thom AS (1981) Turbulence in and above plant canopies. Annu Rev Fluid Mech 13(1):97–129

Reynolds RT, Castro IP (2008) Measurements in an urban-type boundary layer. Exp Fluids 45(1):141–156

Rossby CG, Montgomery RB (1935) The layer of frictional influence in wind and ocean currents. Pap Phys Oceanogr Meteorol 3(3):1–101

Roth M (2000) Review of atmospheric turbulence over cities. Q J R Meteorol Soc 126(564):941–990

Shinn JH (1971) Steady-state two-dimensional air flow in forests and the disturbance of surface layer flow by a forest wall. Atmospheric Sciences Lab, White Sands Missile Range, New Mexico

Shockling M, Allen J, Smits AJ (2006) Roughness effects in turbulent pipe flow. J Fluid Mech 564:267–285

Smits AJ, McKeon BJ, Marusic I (2011) High Reynolds number wall turbulence. Annu Rev Fluid Mech 43:353–375

Sogachev A, Kelly M (2016) On displacement height, from classical to practical formulation: stress, turbulent transport and vorticity considerations. Boundary-Layer Meteorol 158(3):361–381

Stull RB (1988) An introduction to boundary-layer meteorology. Kluwer, Dordrecht

Thom A (1971) Momentum absorption by vegetation. Q J R Meteorol Soc 97:414–428

Townsend AA (1980) The structure of turbulent shear flow, 2nd edn. Cambridge University Press, Cambridge, UK

Wieringa J (1993) Representative roughness parameters for homogeneous terrain. Boundary-Layer Meteorol 63(4):323–363

Yee E, Gailis RM, Hill A, Hilderman T, Kiel D (2006) Comparison of wind-tunnel and water-channel simulations of plume dispersion through a large array of obstacles with a scaled field experiment. Boundary-Layer Meteorol 121(3):389–432

Zaki SA, Hagishima A, Tanimoto J, Ikegaya N (2011) Aerodynamic parameters of urban building arrays with random geometries. Boundary-Layer Meteorol 138(1):99–120

Zhu X, Iungo GV, Leonardi S, Anderson W (2017) Parametric study of urban-like topographic statistical moments relevant to a priori modelling of bulk aerodynamic parameters. Boundary-Layer Meteorol 162(2):231–253